Response to CO_2 Transient Increase in the GISS Coupled Model: Regional Coolings in a Warming Climate

GARY L. RUSSELL AND DAVID RIND

Institute for Space Studies, Goddard Space Flight Center, New York, New York

(Manuscript received 17 October 1997, in final form 20 March 1998)

ABSTRACT

The GISS coupled atmosphere–ocean model is used to investigate the effect of increased atmospheric CO_2 by comparing a compounded 1% CO_2 increase experiment with a control simulation. After 70 yr of integration, the global surface air temperature in the 1% CO_2 experiment is 1.43°C warmer. In spite of this global warming, there are two distinct regions, the northern Atlantic Ocean and the southern Pacific Ocean, where the surface air temperature is up to 4°C cooler. This situation is maintained by two positive feedbacks: a local effect on convection in the South Pacific and a nonlocal impact on the meridional circulation in the North Atlantic. The poleward transport of latent energy and dry static energy by the atmosphere is greater in the 1% CO_2 experiment, caused by warming and therefore increased water vapor and greater greenhouse capacity at lower latitudes. The larger atmospheric transports tend to reduce upward vertical fluxes of heat and moisture from the ocean surface at high latitudes, which has the effect of stabilizing the ocean, reducing both convection and the thermohaline circulation. With less convection, less warm water is brought up from below, and with a reduced North Atlantic thermohaline circulation (by 30% at time of CO_2 doubling), the poleward energy transport by the oceans decreases. The colder water then leads to further reductions in evaporation, decreases of salinity at high latitudes, continued stabilization of the ocean, and maintenance of reduced convection and meridional overturning. Although sea ice decreases globally, it increases in the cooling regions, which reduces the overall climate sensitivity, especially in the Southern Hemisphere. Tropical warming has been observed over the past several decades; if modeling studies such as this and others that have produced similar effects are valid, these processes may already be beginning.

1. Introduction

The response of the atmosphere–ocean system to increasing anthropogenic trace gases is the subject of intense scrutiny. Of particular interest is the possibility that within the general environment of warming, ocean circulation or mixing effects can produce locations of minimum warming or actual cooling. The United Nations Intergovernmental Panel on Climate Change (IPCC) in its Second Assessment Report on Climate Change (Houghton et al. 1996) notes that 4 of 15 coupled atmosphere–ocean models that contributed to its assessment produce cooling at high southern latitudes. Eight additional models produce minimal warming there. The IPCC suggests that since these effects occur in regions of deep vertical mixing (i.e., deeper ''mixed layer depths''), it is the distribution of heat over great depths that is the main process involved; it is noted that the effect is missing in a National Center for Atmospheric Research (NCAR) model (Washington and Meehl 1996), which lacks deep mixing at high southern latitudes. Most models also produce minimal warming in the northern Atlantic Ocean, and the Goddard Institute for Space Studies (GISS) model produces actual cooling extending into the Norwegian Sea. Although deep mixing can cause minimal warming by spreading a heat perturbation over more water, only changes in mixing or transport can contribute to actual cooling.

Another feature that occurs in (eight) coupled models is that the North Atlantic thermohaline circulation decreases as climate warms, with decreases varying from 10% to 30%. In the models at the Geophysical Fluid Dynamics Laboratory (GFDL; Manabe et al. 1991), the Max Planck Institute (Cubasch et al. 1992), and the U.K. Meteorological Office, (UKMO; Murphy and Mitchell 1995), the warmer climate is associated with an increase in moisture at high latitudes, reduced salinity and density, and hence less sinking. A similar effect occurred in these models at high southern latitudes. Weakening of the ocean circulation can further inhibit high-latitude warming. Houghton et al. (1996) noted that the circulation changes are missing in models with weak thermohaline circulations for the current climate (e.g., Meteorologic Research Institute, Japan). Although the

Corresponding author address: Dr. Gary L. Russell, NASA/Goddard Institute for Space Studies, 2880 Broadway, New York, NY 10025.
E-mail: russell@giss.nasa.gov

GISS model circulation is weak at its poleward extent, the effect happens anyway, as shown below.

Global warming and increases in moisture have been noted over the past several decades (Houghton et al. 1992, 1996). Levitus et al. (1994, 1995) cited observations that from 1966 to 1990 the northern Atlantic Ocean cooled from the surface down to 125 m. The maximum cooling of 0.5°C decade^{-1} occurred south of Greenland. The cooling extended to the Norwegian Sea where the data stops. If these two effects are related, the changes simulated in coupled atmosphere–ocean models for the next century may already be occurring, although the oceanic trend may be part of an ocean basin oscillation (Sutton and Allen 1997; McCartney 1997). It is therefore important to understand the processes behind the model results.

In this study, we document the differences between a compounded 1% CO_2 increase experiment and a control simulation using the GISS coupled atmosphere–ocean model (Russell et al. 1995). The model produces cooling regions of more than 4°C in the southern Pacific Ocean and northern Atlantic Ocean. The magnitudes of these coolings are enhanced by positive feedbacks on the surface ocean waters, which lead to greater variability.

2. Model and experiments

The GISS coupled atmosphere–ocean model is run at 4° lat × 5° long horizontal resolution, with 9 layers in the atmosphere and up to 13 layers in the ocean. As described in Russell et al. (1995), it has a number of unique features that differentiate it from many other models. The ocean has a free surface allowing divergent mass flow; precipitation and river flow can be added directly to the ocean, maintaining global conservation of energy, water mass, and salt. The mean and three-dimensional gradients of heat, salt, and water vapor are prognostic variables that are advected using the linear upstream scheme (Russell and Lerner 1981). The effective resolution is finer than that advertised because there are four numbers for each quantity and each grid box. A river flow scheme (Miller et al. 1994) directs continental runoff to the proper ocean box with proper time delay for liquid precipitation or snowmelt to reach the ocean. Ocean flow through 12 subresolution straits is accelerated by the pressure gradient force at each end. The atmosphere and ocean react every simulated hour with surface fluxes of the same magnitude but opposite sign.

Neither flux corrections nor restoring forces are used. Thus the model has deficiencies common to ocean models run in these conditions. In particular, the ocean surface temperature is too warm near the east coast of the tropical oceans. The ocean surface salinity is up to 3 mil^{-1} too low in the northern Atlantic Ocean, consistent with weak North Atlantic Deep Water (NADW) production, especially poleward of 45°N. A small ocean temperature climatic drift occurs, of 0.007°C yr^{-1}; in the thermocline region the drift is 0.02°C yr^{-1}. Further details of the model's control simulation are presented in Russell et al. (1995).

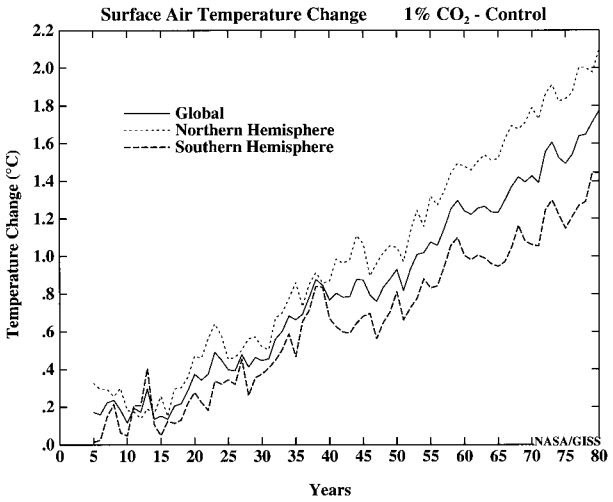

FIG. 1. Change in annual surface air temperature as a function of time, 1% CO_2 experiment minus control simulation.

The ocean currents in the control simulation were initially zero, while ocean temperature and salinity started from Levitus (1982) conditions. As shown in Russell et al. (1995), many processes stabilize after the first 20 yr and remain relatively constant for the next 100 yr. The compounded 1% CO_2 increase experiment is initialized from the control simulation state after 23 yr of integration, during which time a substantial climate drift occurred. Subsequently, the model was relatively stable, especially during the last 50 yr of the runs (see Figs. 4 and 11 below); hence the experiment and control simulation are integrated in parallel for 80 yr following this 23-yr spinup state.

Note that the 1% CO_2 experiment is not an equilibrium simulation. At any time during the experiment there is unrealized warming. Furthermore, since the simulation starts as if the coupled system were in equilibrium, it underestimates the magnitude of the warming to be expected for the first few decades (the ''cold start'' problem).

3. Results

The surface air temperature increases by 1.43°C globally at the time of CO_2 doubling, somewhat more in the Northern Hemisphere (Fig. 1). (Time plot values of experiment minus control are calculated as the experiment value minus a 9-yr average of the control values in order to give the reader the proper sense of interannual variability.) The lack of response for the first several decades is typical of such cold start simulations. One estimate (Hasselmann et al. 1993; Keen 1995) is that the effect of the cold start is to minimize the actual warming by

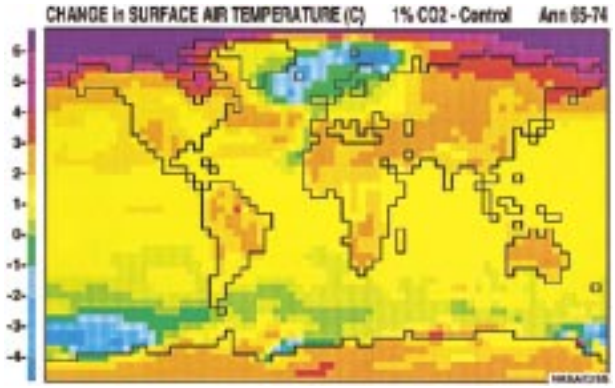

FIG. 2. Change in surface air temperature for years 65–74, at time of CO_2 doubling.

close to 0.5°C by year 70. The global ocean temperature difference as a function of depth at CO_2 doubling time indicates that the warming penetration falls off after the first ~300 m depth, especially in the Northern Hemisphere. The global temperature response y (°C) varies exponentially with depth z (m) as $y = 0.88 \exp(-z/811)$, hence an e-folding depth of 811 m. The correlation coefficient for this function is $r = 0.989$. Modeled as a heat diffusion phenomenon, this is equivalent to a heat diffusion coefficient of about 3.3 $cm^2\ s^{-1}$ at 100-m depth, 2.9 $cm^2\ s^{-1}$ at 300 m. The temperature response is about 20% less than the average shown for atmosphere–ocean general circulation models in Houghton et al. (1996, Fig. 6.4), although the trend is close to the 0.3°C $decade^{-1}$ change associated with a climate sensitivity of 2.5°C for doubled CO_2 estimated by Houghton et al.

The model's free surface allows the thermal expansion of the ocean due to the warming and its distribution with depth to be output directly. After 70 yr sea level from thermal expansion alone rises about 10 cm; if the temperature change correction for the cold start had produced warming 4/3 as large, thermal expansion would have been roughly 13 cm. This is somewhat less than the Houghton et al. (1996) estimated thermal expansion for scenario IS92a of close to 20 cm. A further discussion of sea level change, including the effect of melting glaciers, will be presented elsewhere.

The distribution of surface air temperature change at the time of CO_2 doubling (Fig. 2) shows distinct regions of cooling in the North Atlantic and in the Southern Ocean (especially near the Ross Sea area). These regions are cooling because of a reduction in the convergence of ocean heat transport, as shown in Fig. 3; this explanation is especially true for the North Atlantic region.

The ocean heat convergence is less because of a reduction in North Atlantic Deep Water formation and associated poleward heat transport. The North Atlantic zonally averaged mass streamfunction at its local maximum (28°N, 900 m) is shown in Fig. 4a; note that while the circulation was decreasing in the control run for part

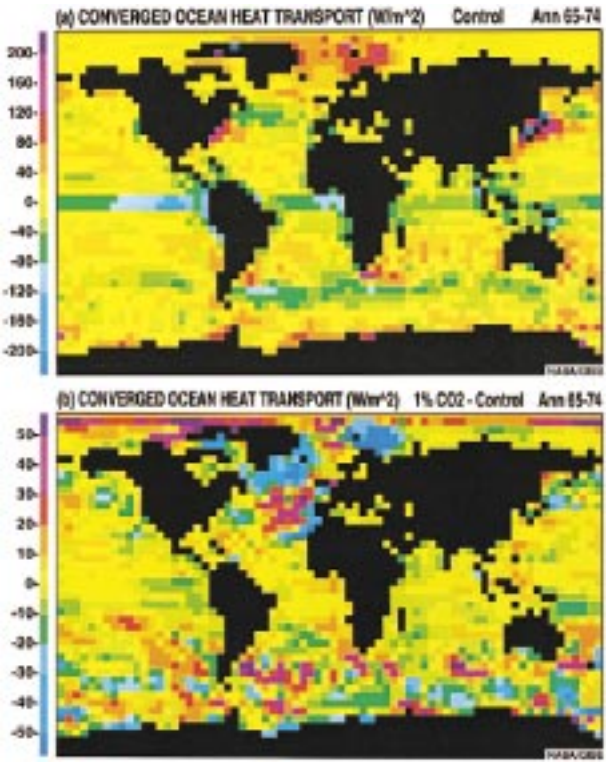

FIG. 3. (a) Converged ocean heat transport in control simulation for years 65–74. (b) Change in converged ocean heat transport for years 65–74, 1% CO_2 experiment minus control simulation.

of this time, the circulation with increased CO_2 was clearly weaker, an effect that set in within the first decade. By the time of the CO_2 doubling, the reduction is close to 30%. The corresponding northward transport of heat in the Atlantic at the same latitude is shown in Fig. 4b. The reduction in heat transport with increased CO_2 occurs throughout much of the time period. Proportionately it is not as great as the streamfunction decrease. Poleward heat transport is also affected by the wind-driven circulation, which actually strengthens somewhat, as the latitudinal temperature gradient increases in the North Atlantic.

Why is this occurring? As CO_2 increases and the globe warms, elevated temperatures lead to greater evaporation and greater retained water vapor, which increases the greenhouse capacity of the atmosphere, especially at low latitudes (because saturation specific humidity is an exponential function of temperature). In contrast the greenhouse capacity increase due to the added CO_2 is relatively independent of latitude. The change in zonally averaged energy transports is shown in Fig. 5. Note that both dry and moist atmospheric poleward energy transports have increased at the time of CO_2 doubling. The atmosphere has responded by transporting more latent heat, due to the added water vapor, and more sensible heat, to higher latitudes where energy is more easily radiated to space. Addition of both

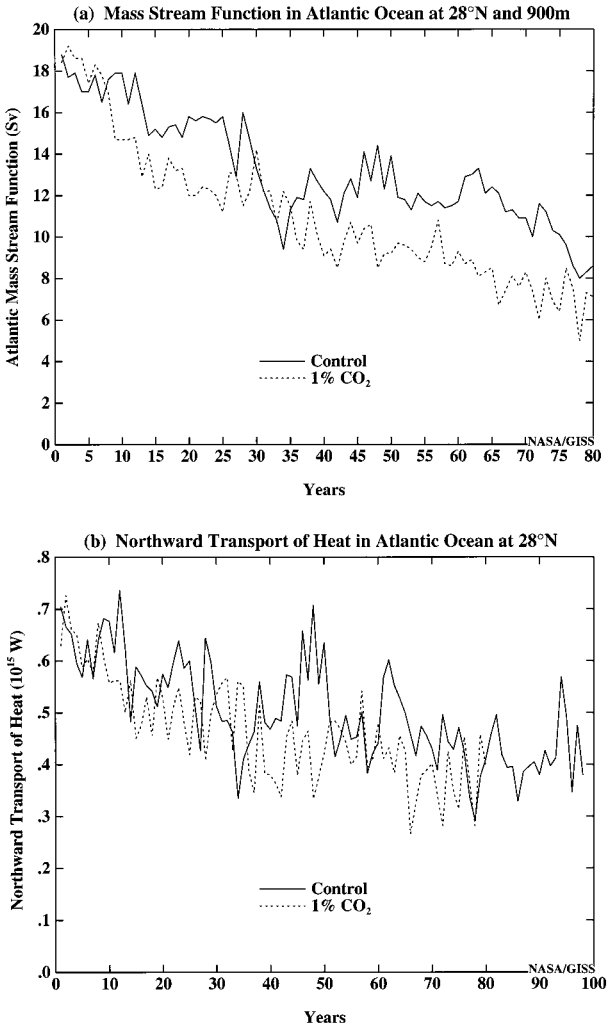

FIG. 4. (a) Annual Atlantic mass streamfunction at 28°N and 900 m as a function of time. (b) Annual northward transport of heat in the Atlantic Ocean at 28°N as a function of time.

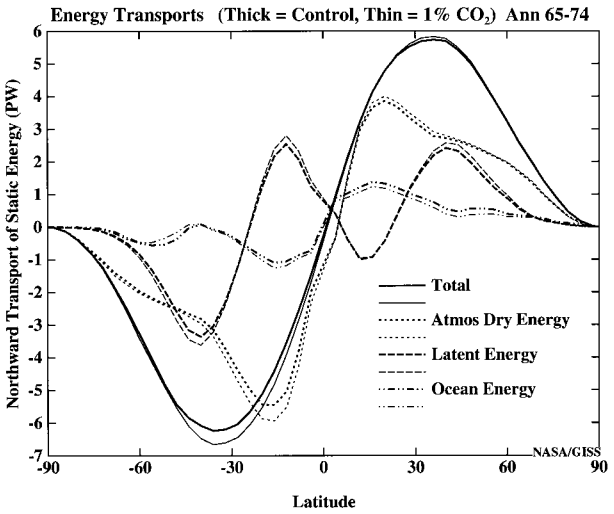

FIG. 5. Northward transport of static energy for years 65–74. Shown are total, dry energy transport (summation of sensible heat plus geopotential energy); latent energy; and ocean energy.

heat and moisture to high latitudes stabilizes the oceans, reducing the thermohaline circulation. Therefore, in response, the ocean heat transport has decreased.

For the North Atlantic cooling region (56–80°N, 35°W–45°E, excluding the Baltic Sea; Fig. 2), the effect of the increase in atmospheric transport of sensible and latent heat is to reduce the upward vertical fluxes of sensible and latent heat into the atmosphere. Shown in Fig. 6a for this region is the change with time of the net heating into the surface, net radiation into the surface, and converged ocean heat transport. The difference of the net heating minus net radiation indicates the change of energy into the ocean by sensible, latent, and precipitation heat fluxes; the positive value beginning around year 30 implies a reduction in ocean energy loss at the surface. This upward vertical flux reduction is in response to the increased moisture and heat transport to high latitudes in the atmosphere, which has the effect of increasing surface layer stability and reducing surface layer heat and moisture gradients between the atmosphere and the ocean, parameters on which the vertical fluxes depend. Since the surface ocean is no longer losing heat and water, its density is decreasing, which reduces the overturning circulation and corresponding oceanic energy transport. Starting with year 39, the converged ocean heat transport is less in the 1% CO_2 experiment than in the control. As the ocean cools in response, sensible and latent heat fluxes decrease further, for colder water will evaporate less moisture and provide less of a vertical temperature gradient at the surface for sensible heat loss. Therefore a positive feedback arises between horizontal ocean heat transport and vertical fluxes, with the overturning circulation acting as the connecting agent.

In the Ross Sea region of the Southern Hemisphere and vicinity (60°–72°S, 165°E–115°W) a similar relationship arises, although as shown in Fig. 3, the converged ocean heat transport change is not as ubiquitous. Whereas in the North Atlantic the reduction in upward vertical fluxes began right from the beginning of the simulation, in this region it did not arise with any consistency until about year 37; the decrease in converged ocean heat transport began about a decade later (Fig. 6b).

The temperature change with time at different ocean depths is shown for these two regions in Figs. 7a,b; note the upper layers are consistently colder for the last 40 yr of the simulation, and so the response at the time of CO_2 doubling (Fig. 1) is not a temporary anomaly. To understand these distributions, we show in Figs. 8a,b the downward heat fluxes at the base of each layer for different processes. In both regions, convection warms the first layer (0–12 m) while cooling layers below.

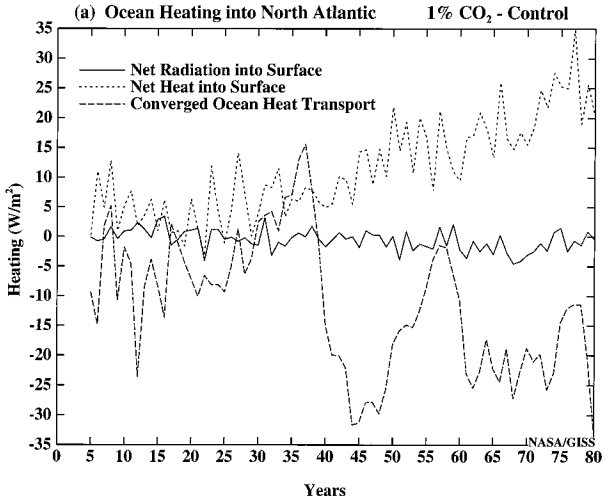

FIG. 6. Change in annual downward net radiation at surface, change in downward net heating at surface (radiation plus surface fluxes), and change in converged ocean heat transport into the (a) North Atlantic cooling region (56°–80°N, 35°W–45°E, except for Baltic Sea), and (b) South Pacific cooling region (60°–72°S, 165°E–115°W).

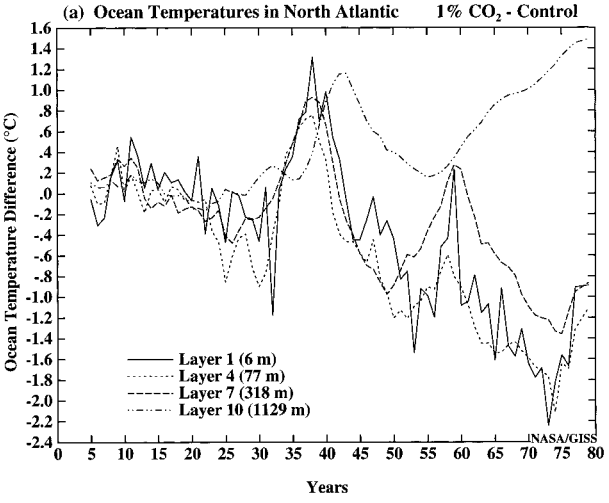

FIG. 7. Change in ocean temperature at different layers on 1 Sep as a function of time for the (a) North Atlantic cooling region, and (b) South Pacific cooling region.

Vertical transport is normally causing warming for the first couple hundred of meters and cooling below.

In the 1% CO_2 experiment in the North Atlantic, while cooling occurs above the thermocline, warming is occurring below (Fig. 7a). Layer 10 (899–1360 m) is warmed by the change in large-scale ocean transports, as both convection and diffusion are nonexistent below layer 9 (Fig. 8a). Reduced convection would tend to warm layers 2 through 7 (12–386 m), but since those layers cooled, convective warming must have been more than compensated by large-scale ocean transport reductions. Hence in this region, the temperature change with depth is dominated by the weakening in the meridional circulation.

In the South Pacific, cooling is occurring only for the first 100 m, with warming below (Fig. 7b). The most significant change below 100 m is the near elimination in the 1% CO_2 experiment of the very deep convection that produced cooling at these depths in the control simulation (Fig. 8b). Now, however, the large-scale circulation transport changes are smaller, so the convective effect predominates. A reduction in horizontal heat flux convergence at all levels, indicative of a reduced thermohaline circulation in this region as well, helps limit the magnitude of the warming below.

Why is convection decreasing in the cooling regions? As the surface temperatures are cooler, and water is warmer at depth, an increase in stability must be the result of salinity changes. As shown in Figs. 9a,b, in both regions, salinity decreases in the first 100 m; the decrease is small at first, and then accelerates some 50 $\pm$ 10 yr into the simulation. This change would account for the decreased convection. Both the salinity decrease and the temperature decrease are larger in the North Atlantic; the effect on the density profile is to minimize

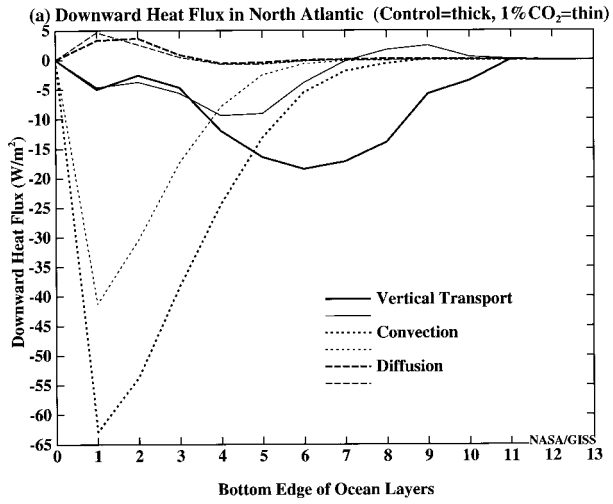

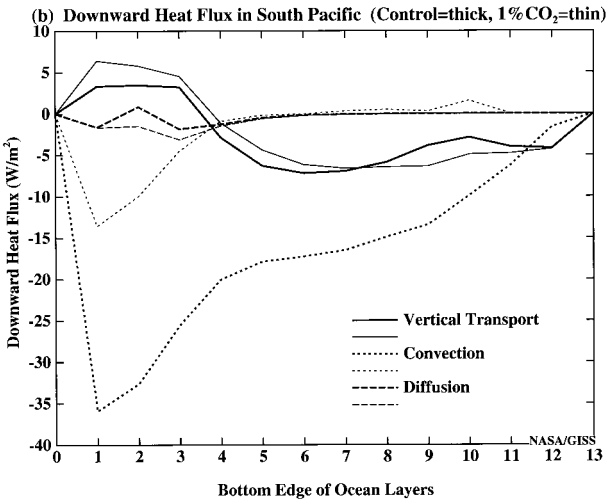

FIG. 8. Downward vertical heat flux for years 65–74 by large-scale vertical ocean transport, ocean convection, and ocean diffusion for (a) North Atlantic cooling region, and (b) South Pacific cooling region. The slope of each curve is equal to the divergence of heat for each layer.

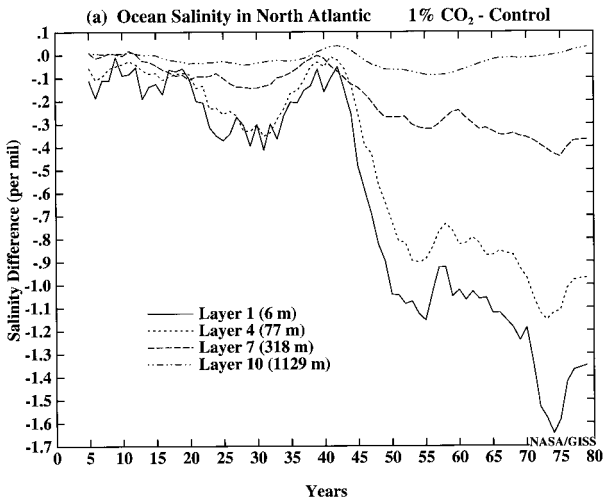

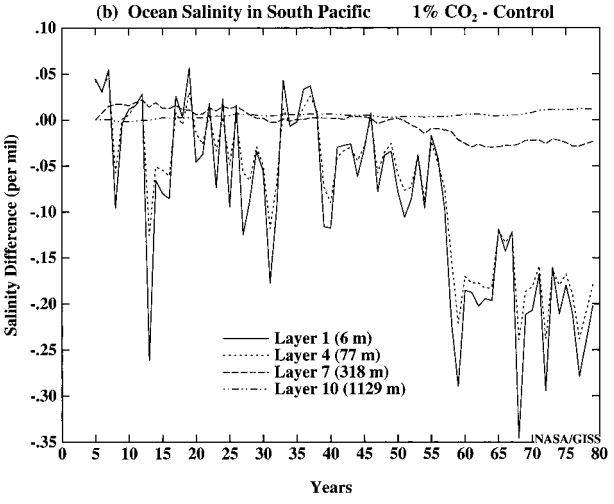

FIG. 9. Change in ocean salinity at different layers on 1 Sep as a function of time for the (a) North Atlantic cooling region, and (b) South Pacific cooling region.

near-surface convection in this region. Deeper convection is being reduced in the Ross Sea area.

Salinity decreases primarily because evaporation decreases (Figs. 10a,b) (although there appears to be some precipitation increase right from the beginning of the simulation in the South Pacific). As the global climate warms, the hydrologic cycle intensifies, and more moisture is carried to high latitudes. Reductions in evaporation occur due to greater atmospheric humidity along with the in situ ocean cooling, therefore becoming more pronounced as the run progresses.

What role is sea ice playing in these effects? Sea ice is parameterized very simply in this version of the model; there is no sea ice advection, and sea ice thermodynamics is handled with a two-layer model. In the North Atlantic cooling region, the control run ice cover oscillates with about a 40-yr period, while in the South Pacific, the control run ice cover starts decreasing some 50 yr into the simulation. In both regions the control run value is somewhat different from observations (Table 1), although there is significant year-to-year variability. These unrealistic aspects of the control run require us to analyze how much of the in situ cooling and evaporation change is due to sea ice effects.

With increased CO_2, the sea ice is greater in both cooling regions, associated with the ocean heat transport reduction and colder temperatures. The increased sea ice reduces vertical fluxes of heat and moisture to the atmosphere (as can be seen from the difference between net heat and net radiation in Fig. 6). Shown in Table 1 are the values for the experiment and control run in years 65–74 for the sea ice cover and the atmosphere–ocean vertical heat fluxes. In the North Atlantic, there is $\sim$20 W m^{-2} reduction in the upward vertical heat flux, most of which is associated with the colder open

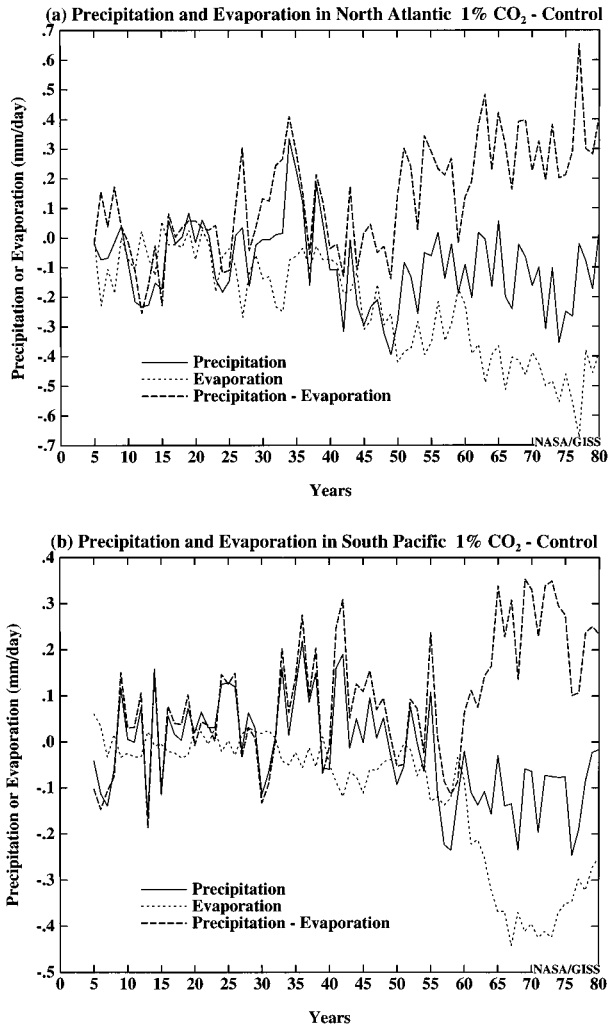

FIG. 10. Change in annual precipitation, evaporation, and precipitation minus evaporation as a function of time for the (a) North Atlantic cooling region, and (b) South Pacific cooling region.

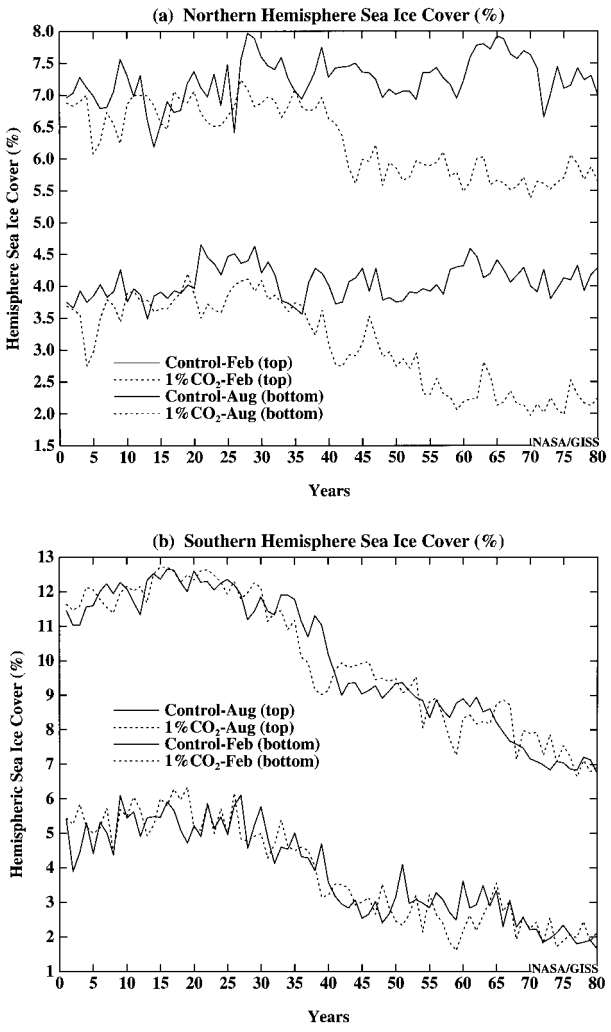

FIG. 11. Ratio of sea ice area to ocean area for Feb and Aug as a function of time for the (a) Northern Hemisphere, and (b) Southern Hemisphere.

ocean waters. The sea ice change, in absolute percentage, is relatively small. In the South Pacific, the upward heat fluxes are reduced by $\sim$16 W m^{-2}, due entirely to the reduction in fluxes in the sea ice region; the open ocean has greater upward fluxes, as the atmosphere is cooling even more than the ocean due to the substantial sea ice increase.

For the planet as a whole, sea ice changes represent a positive feedback on solar radiation and a negative feedback on thermal radiation, with the solar effect normally predominating. In the Northern Hemisphere, sea ice decreases beginning around year 20, with $\sim$25% reduction by year 70 (Fig. 11). In contrast, Southern Hemisphere sea ice shows little reduction. Rind et al.

TABLE 1. Annual sea ice cover, downward surface heat fluxes, and converged ocean heat transport in the North Atlantic and South Pacific cooling regions, years 65–74. Observations from the Atmospheric Model Intercomparison Project (Gates 1992).

North Atlantic	Control	Expt	South Pacific	Control	Expt
Sea ice cover (%)	4.23*	12.09	Sea ice cover (%)	45.56**	73.86
Open ocean fluxes (W m^{-2})	−44.79	−27.10	Open ocean fluxes (W m^{-2})	−46.98	−54.77
Sea ice region fluxes (W m^{-2})	15.04	17.13	Sea ice region fluxes (W m^{-2})	12.63	14.96
Composite fluxes (W m^{-2})	−42.26	−21.75	Composite fluxes (W m^{-2})	−19.82	−3.27
Converged ocean heat transport (W m^{-2})	45.23	21.60	Converged ocean heat transport (W m^{-2})	19.37	15.18

* Observed value = 13.2%.
** Observed value = 33.4%.

(1995) found that when sea ice was not allowed to change, the effect influenced both hemispheres; the Southern Hemisphere temperature response was 40% less than that for the Northern Hemisphere (Fig. 1).

4. Discussion and conclusions

As in the case of other models, the GISS coupled atmosphere–ocean model response to increased CO_2 is to produce regions of large temperature change discrepancy. As noted in the introduction, Houghton et al. (1996) explained the effect as due to 1) sequestering of heat at depth in regions of deep water formation, reducing the surface warming, and 2) reduction in the large-scale ocean circulation resulting in reduced heat transports and actual cooling. A third effect must be added: changes in convection. The first effect can contribute to minimizing the warming, but it cannot cause actual cooling. The GISS model results exemplify the second and third explanations, in that changes in ocean circulation and convection are resulting in the cooling noted in two specific regions. Both effects contribute to both cooling regions, but reductions in converged ocean heat transport dominate the North Atlantic cooling while reductions in convection dominate the South Pacific cooling. The summation of downward surface fluxes plus converged ocean heat transports is negative in the North Atlantic cooling region but positive in the South Pacific.

Two types of positive feedbacks are occurring which produce the observed effect. The first, a local feedback, arises by the influence of salinity on ocean convection. Incrementally colder surface water leads to reduced evaporation, reduced salinity, greater stability, less convection, and less raising of warm water at depth to the surface. This process is exemplified by the southern Pacific cooling region.

The second feedback is nonlocal. The meridional cells and ocean heat transport decrease in response to increased atmospheric transports of dry and moist energy. The atmospheric response is a direct consequence of the greater water vapor content and its added greenhouse capacity particularly at tropical and subtropical latitudes. Relative to the control run, the 1% CO_2 increase experiment radiates energy to space more easily from high latitudes than from low latitudes because the greenhouse capacity of water vapor increases less in high latitudes than it does in low latitudes. The increased horizontal atmospheric transports then reduce the upward vertical fluxes of heat and moisture from the surface, increasing the salinity and stabilizing the ocean at high latitudes. The more stable ocean leads to reductions in the thermohaline circulation, and the cooling regions occur where the weaker ocean heat transports converge less heat. The colder water then produces further reductions in evaporation. Note that the North Atlantic thermohaline circulation decrease of 30% is in agreement with the estimate derived by Stocker and Schmittner (1997) from a simplified basin model *despite* their conclusion that the North Atlantic would be both fresher and *warmer*. This is true as a whole, but not in the cooling regions.

It is interesting to note that the two feedbacks noted in this context, advection and convection, have also been suggested as potential causes for multiple equilibria in the ocean circulation (Lenderink and Haarsma 1994; Rahmstorf 1994). In the 1% CO_2 experiment, these processes are responsible for providing cooling at the surface and weakening the overturning circulations, effects maintained in a similar manner to the possible maintenance of multiple equilibria. However, actual cooling is not necessary to produce a weakened circulation, as it occurs in models with only minimized warming in the North Atlantic (Houghton et al. 1996).

How likely are these changes to occur in the real world? To the extent that the process is initiated by increased warming at low and subtropical latitudes, it obviously depends upon the actual climate sensitivity of these regions. The magnitude of the tropical–subtropical warming is somewhat atmospheric model dependent (Rind 1987); however, an early tropical response occurs in a wide variety of models, including those with reduced tropical warming for doubled CO_2 (Manabe et al. 1991). An ''ENSO-like'' mean climate change response from increased CO_2 has been noted in different coupled models (Knutson and Manabe 1995, 1998; Tett 1995; Meehl and Washington 1996), and an indication of that can be seen here as well (Fig. 2); for whatever it is worth, there has been an increased frequency of El Niños during the 1990s. Nevertheless, the proper tropical climate sensitivity is still in doubt (Rind 1995). Were the tropical atmosphere to warm, a rapid oceanic response is likely to be real, driven by the relatively small mixed layer depths and vertical mixing found at low latitudes.

The reality of the modeled deep water change is more problematic. The model's NADW in the control run peaks somewhat equatorward of observed values, and, at the time of CO_2 doubling, somewhat reduced values (11 Sv at $\sim 28^\circ$N). A stronger circulation originating farther north might respond differently; however, the range of models that have roughly similar responses, with and without flux corrections, seems to imply that a certain generality applies regardless of the precise fidelity of the control run simulation (e.g., Houghton et al. 1996; Gregory and Mitchell 1997).

Why is the GISS coupled model the only one surveyed by Houghton et al. (1996) that shows actual cooling in the northern Atlantic? Its reduction in ocean poleward heat transport must be either more extreme or more localized. The streamfunction reduction of about 30% is similar to some of the model results noted in Houghton et al. (1996) (e.g., GFDL, UKMO). The GISS coupled model is probably the only model that does not incorporate explicit horizontal diffusion of heat and salt. The linear upstream scheme (Russell and Lerner 1981)

for the advection of heat and salt allows for sharper gradients for those quantities, which may help localize the effect.

Other processes that might impact these results are sea ice formation and freshwater input at high southern latitudes, which are handled crudely in this version of the model. The evaporation and salinity change at high southern latitudes is strongly associated with the modeled sea ice change and lack of sea ice advection. A more realistic sea ice parameterization might alter the results, in both hemispheres. The increase of sea ice in the cooling regions lowers the model's sensitivity to the 1% CO_2 increase; in fact, the GISS coupled model has one of the lowest sensitivities of those cited by Houghton et al. (1996). A newer version of the model in which these aspects are treated more realistically is being developed, and these experiments will be repeated to determine their sensitivity to the model formulation.

Perhaps coincidentally, or perhaps not, tropical warming has occurred at almost all longitudes over the past several decades (Houghton et al. 1996). If the resultant model responses are correct, deep water reductions should soon be initiated, if not already occurring. As noted above, the North Atlantic has been cooling at 125-m depth for the last several decades (Levitus et al. 1994, 1995). Observations of modest sea ice increases in the Ross Sea (Stammerjohn and Smith 1997) are also consistent with the changes described here. Perhaps the coupled model's projected ocean changes are beginning to occur.

Acknowledgments. Investigation of the high-latitude response to climate change is funded by NASA Polar Programs. Atmospheric climate modeling at GISS is funded by the NASA Climate Program.

REFERENCES

Cubasch, U., K. Hasselmann, H. Hock, E. Maier Reimer, U. Mikolajewicz, B. D. Santer, and R. Sausen, 1992: Time-dependent greenhouse warming computations with a coupled ocean–atmosphere model. *Climate. Dyn.,* **8,** 55–69.

Gates, L., 1992: AMIP: The Atmospheric Model Intercomparison Project. *Bull. Amer. Meteor. Soc.,* **73,** 1962–1970.

Gregory, J. M., and J. F. B. Mitchell, 1997: The climate response to CO_2 of the Hadley Centre coupled AOGCM with and without flux adjustment. *Geophys. Res. Lett.,* **24,** 1943–1946.

Hasselmann, K., R. Sausen, E. Maier-Reimer, and R. Voss, 1993: On the cold start problem in transient simulations with coupled atmosphere–ocean models. *Climate Dyn.,* **9,** 53–62.

Houghton, J. T., B. A. Callander, and S. K. Varney, Eds., 1992: *Climate Change 1992: The Supplementary Report to the IPCC Scientific Assessment.* Cambridge University Press, 200 pp.

——, L. G. Meira Filho, B. A. Callander, N. Harris, A. Kattenberg, and K. Maskell, Eds., 1996: *Climate Change 1995: The Science of Climate Change.* Cambridge University Press, 567 pp.

Keen, A. B., 1995: Investigating the effects of initial conditions on the response of the Hadley Centre Coupled Model. Hadley Centre Internal Note 71. [Available from Hadley Centre for Climate Prediction and Research, Meteorological Office, London Rd., Bracknell, Berkshire RG12 2SY, United Kingdom.]

Knutson, T. R., and S. Manabe, 1995: Time-mean response over the tropical Pacific due to increased CO_2 in a coupled ocean–atmosphere model. *J. Climate,* **8,** 2181–2199.

——, and ——, 1998: Model assessment of decadal variability and trends in the tropical Pacific Ocean. *J. Climate,* **11,** 2273–2296.

Lenderink, G., and R. J. Haarsma, 1994: Variability and multiple equilibria of the thermohaline circulation associated with deep-water formation. *J. Phys. Oceanogr.,* **25,** 2547–2560.

Levitus, S., 1982: *Climatological Atlas of the World Oceans.* NOAA Prof. Paper 13, 173 pp. [Available from U.S. Goverment Printing Office, Washington, DC 20402.]

——, J. I. Antonov, and T. P. Boyer, 1994: Interannual variability of temperature at a depth of 125 meters in the North Atlantic Ocean. *Science,* **266,** 96–99.

——, ——, Z. Zhou, H. Dooley, V. Tereschenkov, K. Selemenov, and A. F. Michaels, 1995: Decadal-scale variability of the North Atlantic Ocean. *Natural Climate Variability on Decade-to-Century Time Scales,* D. G. Martinson, K. Bryan, M. Ghil, M. M. Hall, T. M. Karl, E. S. Sarachik, S. Sorooshian, and L. D. Talley, Eds., National Academy of Science Press, 318–324.

Manabe, S., R. J. Stouffer, M. J. Spelman, and K. Bryan, 1991: Transient responses of a coupled ocean-atmosphere model to gradual changes of atmospheric CO_2. Part I: Annual mean response. *J. Climate,* **4,** 785–818.

McCartney, M., 1997: Is the ocean at the helm? *Nature,* **388,** 821–822.

Meehl, G. A., and W. M. Washington, 1996: El Niño-like climate change in a model with increased atmospheric CO_2 concentrations. *Nature,* **382,** 56–60.

Miller, J. R., G. L. Russell, and G. Caliri, 1994: Continental-scale river flow in climate models. *J. Climate,* **7,** 914–928.

Murphy, J. M., and J. F. B. Mitchell, 1995: Transient response of the Hadley Centre Coupled Model to increasing carbon dioxide. Part II: Temporal and spatial evolution of patterns. *J. Climate,* **8,** 57–80.

Rahmstorf, S., 1994: Rapid climate transitions in a coupled ocean–atmosphere model. *Nature,* **372,** 82–85.

Rind, D., 1987: The doubled CO_2 climate: Impact of the sea surface temperature gradient. *J. Atmos. Sci.,* **44,** 3235–3268.

——, 1995: Drying out at the tropics. *New Sci.,* **146,** 36–40.

——, R. Healy, C. Parkinson, and D. Martinson, 1995: The role of sea ice in 2 × CO_2 climate model sensitivity. Part I: The total influence of sea ice thickness and extent. *J. Climate,* **8,** 449–463.

Russell, G., and J. Lerner, 1981: A new finite differencing scheme for the tracer transport equation. *J. Appl. Meteor.,* **20,** 1483–1498.

——, J. R. Miller, and D. Rind, 1995: A coupled atmosphere–ocean model for transient climate change studies. *Atmos.–Ocean,* **33,** 683–730.

Stammerjohn, S. E., and R. C. Smith, 1997: Opposing southern ocean climate patterns as revealed by trends in regional sea ice coverage. *Climate Change,* **37,** 617–639.

Stocker, T. F., and A. Schmittner, 1997: Influence of CO_2 emission rates on the stability of the thermohaline circulation. *Nature,* **388,** 862–865.

Sutton, R. T., and M. R. Allen, 1997: Decadal predictability of North Atlantic sea surface temperature and climate. *Nature,* **388,** 563–567.

Tett, S., 1995: Simulation of El Nino–Southern Oscillation-like variability in a global AOGCM and its response to CO_2 increase. *J. Climate,* **8,** 1473–1502.

Washington, W. M., and G. A. Meehl, 1996: High latitude climate change in a global coupled ocean–atmosphere–sea ice model with increased atmospehric CO_2. *J. Geophys. Res.,* **101,** 12 795–12 801.